

Open Cell Metal Foams for Beam Liners ?

R.P. Croce, S. Petracca, A. Stabile*

WavesGroup, University of Sannio at Benevento, 82100 Benevento, IT

*arturo.stabile@sa.infn.it

Abstract — The possible use of open-cell metal foams for particle accelerator beam liners is considered. Available materials and modeling tools are reviewed, potential pros and cons are pointed out, and a study program is outlined.

1. INTRODUCTION

Molecular gas desorption from the beam-pipe wall due to synchrotron radiation should be properly taken into account in the design of high energy particle accelerators and storage rings. This is specially true for hadron colliders, where nuclear scattering in the residual gas, besides limiting the beam luminosity lifetime, may produce high energy protons causing thermal runaway and quenching of superconducting magnets.

In the CERN Large Hadron Collider [1] a copper-coated stainless-steel beam pipe (or *liner*) is kept at $\approx 20K$ by active Helium cooling, and effectively handles the heat load represented by synchrotron radiation, photoelectrons, and image-charge losses. A large number ($\sim 10^2 m^{-1}$) of tiny slots are drilled in the liner wall (see Figure 1) in order to maintain the desorbed gas densities below a critical level ($\sim 10^{15} molecules/m^3$ for H_2) by allowing desorbed gas to be continuously cryopumped toward the stainless steel cold bore (co-axial to the liner) of the superconducting magnets, which is kept at $1.9K$ by superfluid Helium.

The size, geometry and density of the pumping holes affect the beam dynamics and stability in a way which is synthetically described by the longitudinal and transverse beam coupling impedances [2]. The hole geometry should be chosen so as to minimize the effect of trapped (cut-off) modes, and the hole pattern should be designed so as to prevent the possible coherent buildup of synchrotron radiation in the TEM waveguide limited by the pipe and the cold bore [3].

Open-cell metal foams could be interesting candidate materials for beam liner design. In the following we give a brief review of their properties, and of the pertinent modeling tools, and draw some preliminary conclusions about the pros and cons of their possible use in beam liners.

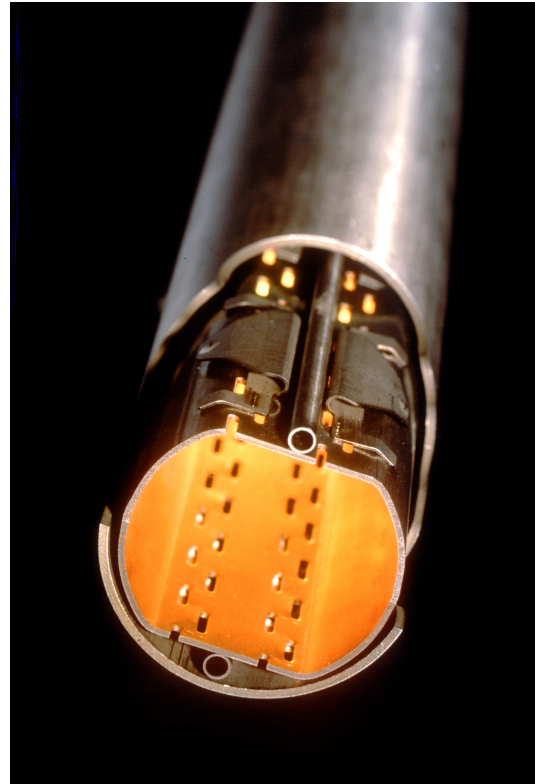


Figure 1: *The LHC slotted copper-plated beam pipe and stainless steel cold bore.*

2. OPEN-CELL METAL FOAMS

Open-cell metal foams are produced either by vapor- (or electro-) deposition of metal on an open-cell polymer template, followed by polymer burn-off, and a final sintering step to densify the ligaments. Alternatively, they are obtained by infiltration/casting of molten metal into a solid mould, consisting of packed (non-permeable) templates of the pores, followed by burn-out and removal of the mould [4]. Both processes result into highly gas-permeable *reticulated* foams, where only a 3D web of solid conducting struts among the pores survives. The typical structure of these materials is displayed in Figure 2. The key structural parameters of reticulated metal foams are the vacuum "pore" size, and the porosity (volume fraction of pores). Pore sizes

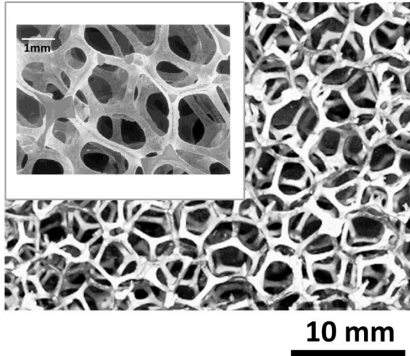


Figure 2: A typical open-cell metal foam structure, at two different viewing scales.

in the range from 10^{-4} to 10^{-3} m and porosities in the range 0.8 - 0.99 are currently manufactured. These two parameters determine the material's gas-permeability, and, together with the electrical properties of the metal matrix, its electrical properties. Metal foams have interesting structural properties (low density and weight, high (tensile and shear)-strength/weight ratio, nearly isotropic load response, low coefficient of thermal expansion), as summarized in Table I, which qualified them among the most interesting new materials for aerospace applications. Aluminum and Copper open-cell foams

	Units	Al	Cu
Compression Strength		2.5	0.9
Tensile Strength		1.2	6.9
Shear Strength		1.3	1.3
Modulus of Elasticity (Compression)	[MPa]	$1 \cdot 10^2$	$7.3 \cdot 10^2$
Modulus of Elasticity (Tension)		$1 \cdot 10^2$	$1 \cdot 10^2$
Shear Modulus		$2 \cdot 10^2$	$2.8 \cdot 10^2$
Specific Heat	[J/g°C]	.89	0.38
Bulk Thermal Conductivity	[W/m°C]	5.8	10.1
Coefficient of Thermal Expansion	[°C ⁻¹]	2.4×10^{-5}	1.7×10^{-5}
Bulk Resistivity	[ohm m]	7.2×10^{-7}	6.5×10^{-7}
Melting Point	[°C]	660	1100

Figure 3: Structural properties of open cell metal foam structure from [5].

are presently available off-the-shelf [5], and are relatively cheap. They can be further coated, e.g., with Silver, Titanium or Platinum, for special purpose applications. Foams using Steel or Brass, as well as pure Silver, Nickel, Cobalt, Rhodium, Titanium or Beryllium have been also produced by a number of Manufacturers.

The Weaire-Phelan (WP) space-filling honeycombs are credited to provide the *natural* (i.e., Plateau's minimal surface principle compliant) model of a reticulated metal with equal-sized (but possibly unequal-shaped) pores [6]. The WP unit cell

consists of a certain arrangement of (irregular) polyhedra, namely two pentagonal-face dodecahedra (with tetrahedral symmetry T_h), and six tetrakaidecahedra (with antiprismatic symmetry D_{2d}) featuring two hexagonal and twelve pentagonal faces. A computer generated WP honeycomb is displayed in Figure 4, and its visual similarity to Figure 2 is apparent.

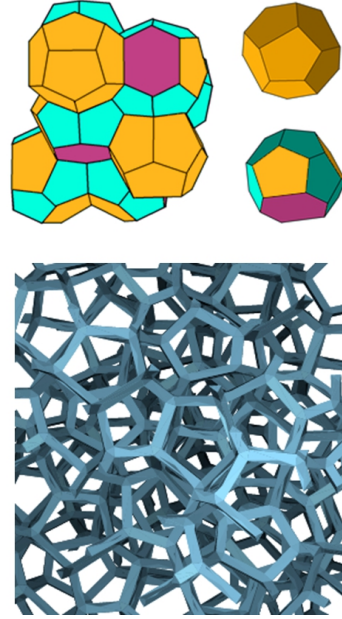


Figure 4: The Weaire-Phelan honeycomb cell (top left), its constituent polyhedra (top right), and a numerically simulated reticulated foam thereof (bottom).

2.1 Electrical Properties of Metallic Foams

Full electromagnetic modeling of reticulated metal foams is still to come. A numerical approach based on Weiland's finite integration technique (FIT, [7]) has been proposed by Zhang et al. [8] to compute the (frequency, thickness and angle of incidence dependent) reflection coefficient of SiC reticulated foam, and optimize its design. A simplified model, consisting of stacked square-mesh grids has been used by Losito et al. [9],[10] to investigate the RF shielding properties of metallic foams.

The main limitation of Zhang's analysis is in the use of a simple body-centered-cubic unit-cell foam model, for easiest numerical implementation. The FIT scheme, however may accommodate in principle more complicated and realistic foam-cell geometries, including in principle the WP one.

In the limit where bubbles and metal struts are much smaller than the smallest wavelength of in-

terest, the DC conductivity of a metal foam can be computed using effective medium theory (EMT), for which several formulations exist (see, e.g., [11]-[13] for a review). These include: i) the infinite dilution approximation, where inclusions do not interact, and are subject to the field which would exist in the homogeneous host; ii) the self-consistent approach [14], credited to Bruggemann, where inclusions are thought of as being embedded in the (yet to be modeled) effective medium; iii) the differential scheme, whereby inhomogeneities are *incrementally* added to the composite¹, until the final concentration is reached, so that at each step the inclusions do not interact, and do not modify the field computed at the previous step [15]; iv) the effective-field methods, whereby interaction among the inclusions is described in terms of an effective field acting on each particle, accounting for the presence of the others. Two main versions of this method exist, credited to Mori-Tanaka [16] and Levin-Kanaun [17], differing in the way the effective field is computed (average over the matrix only, or average over the matrix *and* the inclusions, respectively).

Both the infinite-dilution and the self-consistent approaches yield

$$\sigma_{eff} = \sigma_0(1 - p\nu), \quad (1)$$

where σ_0 is the bulk metal conductivity, p is the porosity (volume fraction of the vacuum bubbles), and ν is a morphology-dependent factor. The differential approach yields

$$\sigma_{eff} = \sigma_0(1 - p)^\nu, \quad (2)$$

while the Mori-Tanaka/Levin-Kanaun approaches yield

$$\sigma_{eff} = \sigma_0 / \left(1 + \frac{\nu p}{1 - p}\right). \quad (3)$$

All equations (1)-(3) merge, as expected, in the $p \rightarrow 0$ limit. The various models are synthetically compared in Figure 5. All these models predict *larger* conductivity than observed in measurements on Al foams². This has been attributed to significant oxide formation on the Al conducting web [18]. Equation (2) agrees in form with predictions based on percolation theory [19] - although strictly speaking there's no threshold here beyond which

¹ In this approach, the total concentration of inhomogeneities does *not* coincide with the volume fraction p , because at each step new inclusions may be placed where old inclusions have already been set.

² It should be noted that open and closed cell metal foams behave similarly in terms of electrical conductivity, while being markedly different as regards thermal conductivity, due to the different role of convective flow.

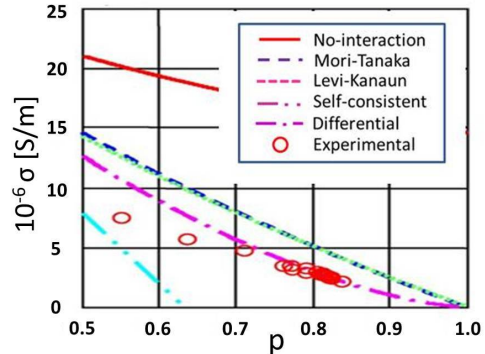


Figure 5: Comparison among different EMT-based reticular foam conductivity models. Static conductivity vs porosity. Aluminum based foam with bulk conductivity $\sigma_0 = 3.5 \cdot 10^7$ S/m. (adapted from [12]).

the conducting component disconnects.

3. METAL FOAMS vs SOLID METAL PERFORATED WALLS

In this section we shall attempt to draw a comparison between a metal-foam beam-pipe wall and a solid-metal perforated one, in terms of the relevant vacuum and beam-coupling impedance features .

3.1 Vacuum Issues

The vacuum dynamics for each molecular species which may be desorbed from the wall by synchrotron radiation can be described by the following set of (coupled) rate equations [20]

$$\begin{cases} V \frac{dn}{dt} = q - an + b\Theta \\ F \frac{d\Theta}{dt} = cn - b\Theta \end{cases} \quad (4)$$

Here n [m^{-3}] and Θ [m^{-2}] are the volume and surface densities of desorbed particles, respectively, and V and F represent the volume and wall-area of the liner per unit length, respectively.

The first term on the r.h.s. of the first rate equation represents the number of molecules desorbed by synchrotron radiation per unit length and time, and is given by

$$q = \eta \dot{\Gamma} \quad (5)$$

where η is the desorption yield (number of desorbed molecules per incident photon) and $\dot{\Gamma}$ is the specific photon flux (number of photons hitting the wall

per unit length and time). The second term represents the number of molecules which are removed per unit time and unit length by either sticking to the wall, or escaping through the holes. The a coefficient in (4) can be accordingly written

$$a = \frac{\langle v \rangle}{4} (s + f) F \quad (6)$$

where $\langle v \rangle \approx (8kT/\pi m)^{1/2}$ is the average molecular speed, m being the molecular mass, k the Boltzmann constant and T the absolute temperature, $\langle v \rangle/4$ is the average number of collisions of a single molecule per unit time and unit wall surface, s is the sticking probability, and f_h is the escape probability. The third term accounts for thermal or radiation induced re-cycling of molecules sticking at the walls. The b coefficient in (4) can be accordingly written

$$b = \kappa \dot{\Gamma} + F \nu_o \exp(-E/kT) \quad (7)$$

Here the first term accounts for radiation induced recycling, described by the coefficient κ [m^2], while the second term describes thermally-activated recycling, ν_o being a typical molecular vibrational frequency, and E a typical activation energy.

The $b\Theta$ term appears with reversed sign on the r.h.s. of the second rate equation, where it represents the the number of molecules *de-sticking* from the wall surface per unit time and unit length. The first term on the r.h.s. of this equation represents the number of molecules sticking to the wall, per unit time and unit length, whence (compare with eq. (6))

$$c = \frac{\langle v \rangle}{4} s F \quad (8)$$

At equilibrium, $\dot{n} = \dot{\Theta} = 0$, and the rate equations yield:

$$\begin{cases} n_{eq} = \frac{4\eta\dot{\Gamma}}{\langle v \rangle f F} \\ \Theta_{eq} = \frac{s}{f} \frac{\eta\dot{\Gamma}}{\kappa\dot{\Gamma} + F\nu_o \exp(-E/kT)} \end{cases} \quad (9)$$

Typical values (from LHC) of the parameters in (9) are collected in Table II below [20]. The equilibrium molecular densities in (9) should not exceed some *critical* values for safe operation [20].

3.1.1 Perforated Solid Metal Wall

For a liner wall with vanishing thickness the escape probability f in (6) and (9) will be simply equal to the holey fraction f_h of the wall surface. For holes drilled in a thick wall, the escape probability will

V	Liner volume (per unit length)	$1.3 \cdot 10^{-3} \text{ m}^3/\text{m}$
F	Liner surface (per unit length)	$0.14 \text{ m}^2/\text{m}$
η	Desorption yield	$5 \cdot 10^{-4}$
$\dot{\Gamma}$	Photon flux (200 mA beam)	$3.14 \cdot 10^{16} \text{ s}^{-1} \text{ m}^{-1}$
σ	Sticking probability	0.6
κ	Recycling coefficient	$5 \cdot 10^{-21} \text{ m}^2$
ν_o	Vibrational frequency	10^{13} s^{-1}
E	Activation energy	0.035 eV/molecule

Figure 6: *Typical values of the parameters in (9) from [20].*

be *less* than f_h , differing from this latter by a factor χ (named after Clausing) which takes into account the nonzero probability that a molecule may stick at the hole *internal* surface rather than escaping outside [21]. The Clausing factor χ for thick cylindrical holes drilled in a metal wall is well approximated by the following empirical formula credited to Iczkowski [22] :

$$\chi = 1 - 0.5(w/R_h) \quad (10)$$

where w and R_h are the thickness and radius of the hole.

3.1.2 Open Cell Metal Foam Wall

For an open cell foam the porosity ρ_h (volume fraction of voids), average pore radius R_h , and volume density of pores N_h are related by:

$$\rho_h \approx \frac{4}{3} \pi R_h^3 N_h \quad (11)$$

which allows to compute N_h from ρ_h and R_h . It is reasonable to assume that the *surface* density of the holes will be $\approx N_h^{2/3}$, each hole having an average surface $\approx (2/3)\pi R_h^2$ so that the fraction of (unit) surface covered by holes will be

$$f_h = 0.806 \cdot \rho_h^{2/3}, \quad (12)$$

which will exceed 60% for a typical (> 0.8) (volume) porosities. This is a *large* number, compared, e.g., to the LHC liner value $f \approx 4.5\%$.

This suggests letting $s \rightarrow s(1 - f_h)$ in eqs. (6) and (9), since molecules can only stick to the *solid* portion of the wall surface.

On the other hand, not *all* molecules hitting the *holey* portion of the wall will escape, and we may expect a (much) larger Clausing factor, compared to the simple case of (right) cylindrical holes drilled in a thick solid plate³. We may naively assume that the effective number of molecules (per unit time

³ The gas-permeability of metal foams has been investigated since long, both experimentally [23] and theoretically (see, e.g., [24] for a recent account). Unfortunately, little attention has been paid so far to the molecular flow limit.

and length) which will *escape* from a metal-foam wall with thickness w , will be related to the number (per unit time and length) of those entering the face-holes by a Lambert-Beers factor, so that

$$f = f_h \exp(-w/\ell), \quad (13)$$

reflecting the fact that those molecules may collide with and stick to the (inner) metal web, instead of escaping. The obvious requirement that (13) agrees with (10) in the $w \rightarrow 0$ limit yields $\ell = 2R_h$ as an estimate of the extinction length in (13).

Note that synchrotron radiation will not penetrate the metal foam beyond a few skin-depths δ_S , so that not *all* molecules sticking to the metal web *inside* the metal foam could be recycled by synchrotron radiation. This implies that the value of the recycling factor κ in (7) and (9) may be significantly different for a reticular wall.

3.2 Beam Coupling Impedance and Parasitic Loss

Beam coupling impedances provide a synthetic description of the beam-pipe interaction, for investigating beam dynamics and stability [2]. For the simplest case of a circular pipe of radius b with on-axis beam, the longitudinal beam-coupling impedance per unit length is given by

$$Z_{\parallel}(\omega) = \frac{Z_{wall}}{2\pi b} \quad (14)$$

where Z_{wall} is the wall impedance, and a Leontóvich assumption is implied⁴. Similarly, the nonzero components of the diagonal transverse beam coupling impedance dyadic are

$$Z_{\perp}(\omega) = \frac{cZ_{wall}}{\omega\pi b^3} \quad (15)$$

where c is the speed of light in vacuum. The parasitic loss (energy lost by the beam per unit pipe length) is directly related to the longitudinal impedance via

$$\Delta\mathcal{E} = \frac{1}{2\pi} \int_{-\infty}^{+\infty} |I(\omega)|^2 \Re Z_{\parallel}(\omega) d\omega. \quad (16)$$

where $I(\omega)$ is the beam-current frequency spectrum [2]. The beam coupling impedances (and parasitic losses) should not exceed some critical values for safe operation [1].

⁴ Equation (14) is a special case of a general formula which allows to compute the longitudinal and transverse beam-coupling impedances of a pipe with complicated geometric and constitutive properties [25].

3.2.1 Perforated Solid Metal Wall

The wall impedance for a perfectly conducting perforated beam pipe was deduced in [26] and [27] in the Bethe limit where the hole size is much smaller than the (shortest) wavelength of interest, yielding

$$\text{Im}[Z_{\parallel}] = -j \frac{Z_0}{2\pi b} \left(\frac{\omega}{c}\right) (\alpha_e + \alpha_m) n_{\sigma}. \quad (17)$$

$$\text{Re}[Z_{\parallel}] = \frac{Z_0}{12\pi^2 b} \left(\frac{\omega}{c}\right)^4 (\alpha_e^2 + \alpha_m^2) n_{\sigma} \quad (18)$$

where $\alpha_{e,m}$ are the electric and magnetic hole polarizabilities, and n_{σ} is the surface density of holes. For circular holes with radius R_h in a wall with thickness w one has, e.g.,

$$\begin{cases} \alpha_e = \frac{2}{3} r_0^3 \exp(-\xi_E w/R_h), \\ \alpha_m = -\frac{4}{3} r_0^3 \exp(-\xi_H w/R_h) \end{cases} \quad (19)$$

where $\xi_E \approx 2.405$ and $\xi_H \approx 1.841$ are the longitudinal damping constants of the dominant TE and TM cutoff mode of a circular waveguide having the same radius r_0 as the holes. Equation (18) can be used in (16) to compute the parasitic loss due to the synchrotron radiation leaking through the holes. The parasitic loss due to the finite bulk conductivity of the liner wall, can also be obtained from (16) using

$$Z_{wall} = \left(\frac{\omega\mu_0}{\sigma}\right)^{1/2} \exp(j\pi/4) \quad (20)$$

in (14).

3.2.2 Open Cell Metal Foam Wall

The wall impedance of a reticular metal is given by (20), in terms of the *effective* conductivity σ_{eff} of the material. Equations (14) and (15) give the corresponding beam coupling impedances, and equation (16) yields the related parasitic loss.

Heuristically, we can also use the skin depth of the reticular metal (evaluated at the frequency of the synchrotron radiation ω_s)

$$\delta_S = \left(\frac{2}{\omega_s \mu_0 \sigma_{eff}}\right)^{1/2} \quad (21)$$

to set the thickness w of the open-cell metal-foam wall, and estimate the fraction of parasitic loss due to synchrotron radiation leakage as

$$\Delta\mathcal{E}^{(rad)} \approx \Delta\mathcal{E} \exp(-2w/\delta_S). \quad (22)$$

4. CONCLUSIONS

On the basis of the above hints, some preliminary qualitative conclusions can be drawn about the possible use of reticular metals in beam liners.

The structural properties of the material may be adequate to resist to eddy-current induced stresses, in case of superconducting magnets' failure.

For a given out-gassing capacity, a smaller total surface of reticular metal may be needed, thanks to the much larger gas permeability of open-cell metal foams in the molecular-flow regime, compared to perforated solid-metal. At the same time, synchrotron radiation leakage could be lower, due to better EM shielding properties, and the risk of coherent beaming of synchrotron radiation in the TEM region between the outer liner wall and the cold bore would be reduced, due to the almost random hole pattern.

Bulk ohmic losses in reticular metals, on the other hand, may be much larger compared to solid metals. This could be mitigated to some extent by coating the metallic web, e.g., with a superconducting material.

Using, e.g., relatively larg(er) holes/slots in the beam-liner, backed by metal foam strips could possibly cope with the very stringent vacuum and impedance requirements of the perspective SLHC [28].

In order to translate the above hints into quantitative design criteria, further modeling effort and substantial experimental work are obviously in order.

We believe that such a study program is worth being pursued, and that the available modeling tools and technologies provide a good starting point for its successful implementation. We are accordingly preparing a research proposal on the subject to be submitted to the Italian National Institute for Nuclear Physics Research (INFN).

References

- [1] - "The Large Hadron Collider Conceptual Design," CERN Rept. AC/95-05 (1995).
- [2] B.W. Zotter and S.A. Kheifets, "Impedances and Wakes in High Energy Particle Accelerators," World Scientific, Singapore (1998).
- [3] S. Heifets and A. Mikhailichenko, "Coherent Synchrotron Radiation in Multiply Connected Vacuum Chamber," SLAC Pub. 8428 (2000).
- [4] J. Banhart and N.A. Fleck, "Cellular Metals and Metal Foaming Technology," MIT Press, Boston (2003).
- [5] www.ergaerospace.com
- [6] D. Weaire and R. Phelan, "A Counter-Example to Kelvin's Conjecture on Minimal Surfaces," Phil. Mag. Lett. **69** (1994) 107.
- [7] T. Weiland, "A Discretization Method for the Solution of Maxwells Equations for Six-Component Fields," AEU Int. J. Electr. **C31** (1977) 116.
- [8] H. Zhang et al., "Numerical Predictions for Radar Absorbing Silicon Carbide Foams Using a Finite Integration Technique with a Perfect Boundary Approximation," Smart Mater. Struct. **15** (2006) 759.
- [9] O. Losito et al., "A Wide-Frequency Model of Metal Foam for Shielding Applications," IEEE Trans. EMC-52 (2010) 75.
- [10] G.Monti, L. Catarinucci and L. Tarricone, "New materials for electromagnetic shielding: Metal foams with plasma properties," MOTL **52** (2010) 1700.
- [11] F.G. Cuevas et al., "Electrical Conductivity and Porosity Relationship in Metal Foams," J. Porous. Mater. **16** (2008) 675.
- [12] I. Sevostianov, J. Kovacic and F. Simancik, "Elastic and Electric Properties of Closed Cell Aluminum Foams," Mat. Sci. Eng. **A420** (2006) 87.
- [13] R. Goodall, L. Weber and A. Mortensen, "The Electrical Conductivity of Microcellular Metals," J. Appl. Phys., 100 (2006) 044912.
- [14] D.A.G. Bruggemann, "Berechnung Verschiedener Physikalischer Konstanten von Heterogenen Substanzen," Ann. Phys. **24** (1935) 636.
- [15] R. McLaughlin, "A Study of the Differential Scheme for Composite Materials," Int. J. Eng. Sci. **5** (1977) 237.
- [16] Y. Qui and G.J. Weng, "On the Application of MoriTanaka's Theory Involving Transversely Isotropic Spheroidal Inclusions," Int. J. Eng. Sci. **28** (1990) 1121.
- [17] S.K. Kanaun, "Dielectric Properties of Matrix Composite Materials with High Volume Concentration of Inclusions (Effective Field Approach)," Int. J. Eng. Sci. **41** (2003) 1287.
- [18] T. W. Clyne, Thermal and Electrical Conduction in MMCs, in *Comprehensive Composite Materials*, Elsevier, Amsterdam (2000).
- [19] D. Stauffer and A. Aharony, "Introduction to percolation Theory," Taylor and Francis, London (1992).

- [20] O. Gröbner, "Overview of the LHC Vacuum System," *Vacuum* **60** (2001) 25.
- [21] W. Steckelmacher, "Knudsen Flow 75 Years on: the Current State of the Art for Flow of Rarefied Gases in Tubes and Systems," *Rep. Progr. Phys.* **49** (1986) 1083.
- [22] R.P. Iczkowski, J.L. Margrave and S.M. Robinson, "Effusion of Gases through Conical Orifices," *J. Phys. Chem.* **67** (1963) 229.
- [23] B.R.F. Kendall, "Vacuum Applications of Metal Foams," *J. Vac. Sci. Technol.* **17** (1980) 1385.
- [24] K. Boomsma, D. Poulikakos and Y. Ventikos, "Simulation of Flow through Open Cell metal Foams using an Idealized Periodic Cell Structure," *Int. J. Heat and Fluid Flow* **24** (2003) 825.
- [25] S. Petracca, "Reciprocity Theorem for Coupling Impedance Computation in the LHC Liner.," *Part. Acc.* **50** (1995) 211.
- [26] S.S. Kurennoy, "Couling Impedances of Pumping Holes," *Particle Accel.* **39** (1992) 1.
- [27] S. Petracca, "Beam Coupling Impedances for Perforated Beam Pipes with General Shape from Impedance Boundary Conditions," *Phys. Rev.* **E60** (1999) 6030.
- [28] <http://care-hhh.web.cern.ch/CARE-HHH/LUMI-06/>